

INFLUENCE OF INCREASED SINTERING TIME ON STRUCTURE AND DIELECTRIC BEHAVIOR OF BARIUM LANTHANIDE TITANATES

DALVEER KAUR, S.BINDRA NARANG

Department of Electronics Technology, Guru Nanak Dev University,
Amritsar-142005, Punjab, India

E-mail: sukhleen2@yahoo.com

Submitted December 03, 2009; accepted February 23, 2010

Keywords: Ceramics, X-Ray diffraction, Scanning electron microscopy, Dielectric properties

Three series of polycrystalline ceramics with a compositional formula of $Ba_{6-3x}Ln_{8+2x}Ti_{18}O_{54}$ with Ln (lanthanide) = Sm, Gd and Nd and $x = 0.0 - 0.7$ were synthesized by the standard double sintering ceramic technique. The changes of sintering time ranging from 2 h to 6 h in steps of 1 h were taken into consideration showing its effect on the behavior of the ceramics. X-Ray Diffraction analysis confirmed that the crystal symmetry was same i.e., orthorhombic with a possible space group of Pbam, for all the ceramics of the three series. The lattice parameters increased with increased sintering time. Grain morphology was investigated with the help of Scanning Electron microscopy. Fired densities have been observed to be greatly improved with the raised sintering time. There was a considerable and similar effect on dielectric and conductivity properties, for all the ceramics series, carried out at a frequency of 3.0 GHz at room temperature. Dielectric constants were increased up to the sintering time of 4 h and then tended to saturate for raised sintering time in all series. Moreover, the loss tangent was seen to be decreased remarkably with increased sintering time in all the series. Relationship between density, crystallites size and dielectric properties has been presented.

INTRODUCTION

A continuous trend of miniaturization in the field of ceramics dielectrics requires higher and higher volumetric efficiencies, which can be realized in two ways including raising of dielectric constants and reduction of losses. For the effectively modified BaTiO₃ dielectrics by doping with various lanthanides (Ln), the largest commercial applications are positive temperature coefficient resistors (PTCRs) [1, 2], luminescence and display materials [3], multilayer ceramic capacitors [4, 5], dielectric resonators [6, 7], etc. In the microwave frequency range, BaTiO₃ dielectrics doped with Ln = Sm, Gd, Eu, Pr, La, Nd, Ho, Er, Dy having a compositional formula $Ba_{6-3x}Ln_{8+2x}Ti_{18}O_{54}$, known as Barium Lanthanide Titanates (BLT), are, to date, the most promising candidates for the synthesis of new high dielectric constant (~ 75-140) ceramics [7-13]. BLTs possess a structure of tetragonal tungsten bronze, which also includes elements of perovskite structure [14, 15]. Within the network of corner sharing TiO₆ octahedra, three types of structural sites in the complex A-sublattice exist: pentagonal sites filled with Ba²⁺ ions, tetragonal sites shared by Ba²⁺ and Ln³⁺ ions, and empty trigonal sites. In BLTs, the electro physical characteristics are related to the grain

sizes, unit-cell volume and the magnitude of octahedral tilting, which decrease with r_A [14]. Moreover, the electro physical properties of microwave dielectrics also depend on many processing parameters including the sintering aids, chemical composition, microstructure and the prepared conditions. The effect of sintering (holding) time on the dielectric properties of many microwave dielectric ceramics is closely related to crystallite size [16]. Actually, the heat treatment of microwave dielectric materials usually require modification of hold times to accommodate heat and mass transfer to achieve exceptionally dense oxides where gas entrapment can dominate final stage removal of porosity. Furthermore, densification is sensitive to the grain size and the attachment of pores to grain boundaries. Any atmosphere trapped in the pores will inhibit densification. An improper firing schedule may introduce pores, inhomogenities, flaws such as blistering or cracking due to binder burn out, etc. So, the sintering time is considered an important parameter for improving the quality of dielectrics, because it is one of the factors that gives rise to the final microstructure and thus control properties and performance of the final product. Only a few papers have been published about the influence of increasing sintering time on the values of dielectric constant (ϵ'), loss tangent ($\tan\delta$) [17, 18].

In the present work, we tried to find out a correlation between the sintering time and dielectric properties. An effort has been made to work out the impact of longer sintering time on the dielectric properties.

EXPERIMENTAL

$Ba_{6-3x}Ln_{8+2x}Ti_{18}O_{54}$ polycrystalline samples with Ln (lanthanide) = Sm, Gd and Nd and $x = 0.0-0.7$ were synthesized by the standard double sintering ceramic technique, using high purity (> 99 %) oxides and carbonates: Sm_2O_3 , Gd_2O_3 , Nd_2O_3 , Ba_2CO_3 and TiO_2 . The stoichiometric mixtures of all the ingredients were thoroughly mixed in wet medium (methanol) for 12 h in an agate mortar and pestle to get a homogeneous mixture. Compounds were dried, ground manually and calcined in high purity alumina crucibles at $1100^\circ C$ for 2 h in an air atmosphere. Calcined powders were again wet milled for 10 h. The fine, homogeneous and calcined powders were then granulated using organic binder polyvinyl alcohol (PVA) to provide strength and flow ability of granules and to reduce the brittleness of the samples. The granulated powders were sieved and compacted in steel dies under a load of 100 MPa. The compacted pellets of the three series were then sintered at $1300^\circ C$ in an oxygen atmosphere for 2 h, 3 h, 4 h, 5 h, 6 h in a linear programmable furnace to burn out organic binder.

For structural analysis X-Ray Diffraction (XRD) spectra were taken on powder samples over a wide range of Bragg angles ($20^\circ < 2\theta < 80^\circ$) at room temperature using a X-ray powder diffractometer (model, Rigaku) with $CuK\alpha$ radiation, $\lambda = 0.15418 nm$ and a scanning rate of $2^\circ(2\theta)/min$. The fractured surfaces of the pellets were

gold coated by a sputtering technique to record the surface morphology of the pellets. Surface morphology was studied by Scanning Electron Microscope (model JSM 6100, JEOL Japan) at room temperature. The sintered pellets were polished by fine emery paper to make both the faces flat and parallel for further characterization. Percentage theoretical density was calculated using XRD data. Microwave dielectric properties were determined using a coaxial probe method with Network Analyzer (model 8714ET, Agilent Technologies) at a frequency of 3 GHz at the room temperature.

RESULTS

The XRD profiles of the three $Ba_{6-3x}Ln_{8+2x}Ti_{18}O_{54}$ series, with $x = 0.6$ and Ln = Sm, Gd, Nd respectively, at the sintering time of 2 h and 6 h, respectively, are shown in Fig. 1a,b. The peak positions of the XRD profiles are shifted to higher 2θ angles (in all the series) with the Ln substitution for Ba. It was observed that both the number of peaks and peak intensity increased with increased sintering time. With the enhanced sintering time, the values of lattice parameters a , b and c increased. The crystal symmetry was orthorhombic for all the series with a possible space group of Pbam No. 55. Systematic shifts of the peaks to the higher 2θ angles indicated a decrease in the lattice parameters with increasing Ln content. In order to clarify the influence of the ionic radii difference between Ba and Ln on the crystal structure, the lattice parameters of the $Ba_{6-3x}Ln_{8+2x}Ti_{18}O_{54}$ compounds were determined based on these X-Ray powder diffraction patterns by least-squares refinement of diffraction data collected with angle recording diffractometer. The results

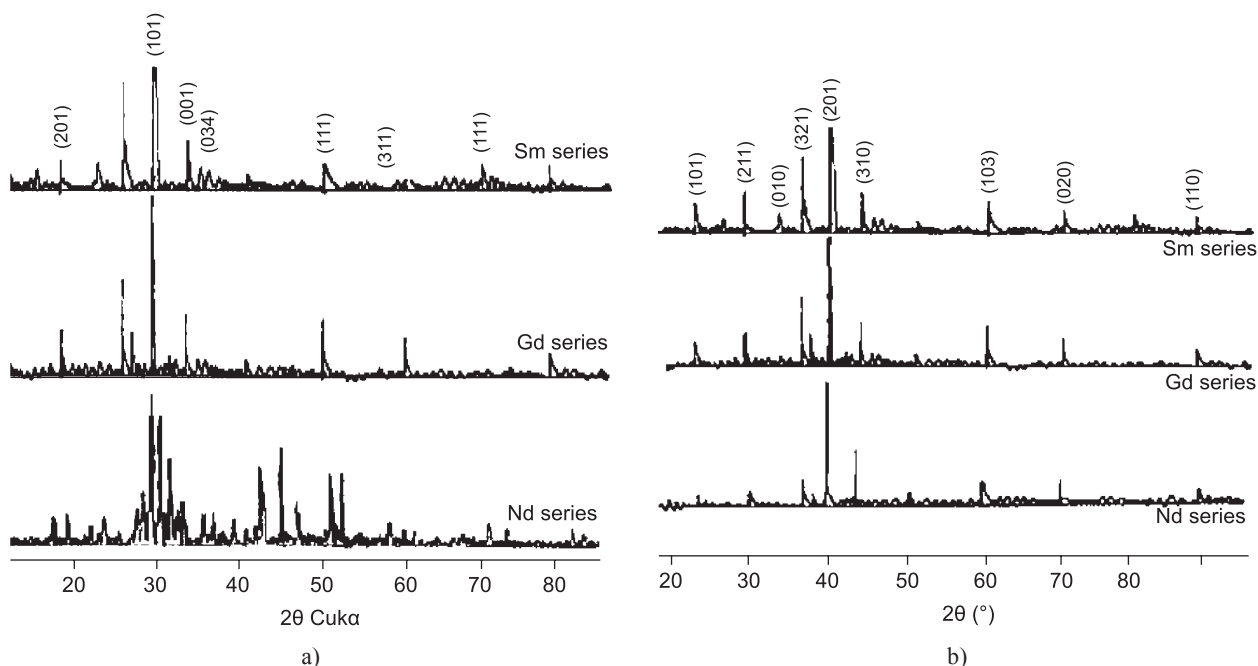


Figure 1. XRD patterns for $Ba_{6-3x}Ln_{8+2x}Ti_{18}O_{54}$ compounds sintered for: a) 2 hours at $1300^\circ C$, b) 6 hours at $1300^\circ C$.

are reported in Tables 1-3 for Sm, Gd and Nd series, respectively, with compounds sintered at 2 h and 6 h for all the compositions. Moreover, for these series, the lattice parameter changes were observed to be quite similar, i.e., a maximum change was found for the b-axis and a minimum for the c-axis. With respect to the changes per Å, the minimum change was 0.28 %, 0.27 % and 0.24 % for the c-axis and the $Ba_{6-3x}Sm_{8+2x}Ti_{18}O_{54}$, $Ba_{6-3x}Nd_{8+2x}Ti_{18}O_{54}$ and $Ba_{6-3x}Gd_{8+2x}Ti_{18}O_{54}$ respectively, with a maximum of 0.39 %, 0.41 % and 0.42 % for the a-axis with the same order, but 0.36 %, 0.35 % and 0.34 % respectively, for the b-axis.

The densification behavior of the compounds with respect to sintering time is plotted in fig. 2a-c for Sm, Gd and Nd series, respectively, for all the compositions. It was observed that the percentage theoretical density greatly improved with increased sintering time. Maximum values have been obtained at the sintering time of 6 h. It was observed to be above 95 % for Sm series 93 % for Gd series and 97 % for Nd series.

Fig. 3a-c illustrates the SEM micrographs of $Ba_{6-3x}Ln_{8+2x}Ti_{18}O_{54}$ compounds with $x = 0.6$ and $Ln = Sm, Gd$ and Nd , respectively. For Sm series, in fig. 3a, irregular shaped randomly distributed grains were observed in

Table 1. Ceramic compositions and variation of Lattice constants with sintering times of 2 h and 6 h, respectively for $Ba_{6-3x}Sm_{8+2x}Ti_{18}O_{54}$ compounds with $x = 0.0-0.7$ at 1300°C.

x	Ceramic composition	Lattice Constants					
		2 h			6 h		
		a	b	c	a	b	c
0.0	$Ba_{6.0}Sm_8Ti_{18}O_{54}$	12.51006	22.2315	3.8163	12.6143	22.3182	3.9282
0.1	$Ba_{5.7}Sm_{8.2}Ti_{18}O_{54}$	12.50983	22.2275	3.8146	12.6129	22.3012	3.9119
0.2	$Ba_{5.4}Sm_{8.4}Ti_{18}O_{54}$	12.50761	22.2087	3.8149	12.6027	22.3001	3.9102
0.3	$Ba_{5.1}Sm_{8.6}Ti_{18}O_{54}$	12.49105	22.2018	3.8171	12.6002	22.2937	3.9072
0.4	$Ba_{4.8}Sm_{8.8}Ti_{18}O_{54}$	12.45831	22.2012	3.8219	12.5939	22.2910	3.8929
0.5	$Ba_{4.5}Sm_{9.0}Ti_{18}O_{54}$	12.32983	22.2011	3.8221	12.5901	22.2901	3.8911
0.6	$Ba_{4.2}Sm_{9.2}Ti_{18}O_{54}$	12.28393	22.2013	3.8239	12.5878	22.2893	3.8901
0.7	$Ba_{3.9}Sm_{9.4}Ti_{18}O_{54}$	12.23722	22.2010	3.8218	12.5812	22.2839	3.8878

Table 2. Ceramic compositions and variation of Lattice constants with sintering times of 2 h and 6 h, respectively for $Ba_{6-3x}Sm_{8+2x}Ti_{18}O_{54}$ compounds with $x = 0.0-0.7$ at 1300°C.

x	Ceramic composition	Lattice Constants					
		2 h			6 h		
		a	b	c	a	b	c
0.0	$Ba_{6.0}Sm_8Ti_{18}O_{54}$	13.5228	21.772	3.7897	13.5428	22.004	4.1387
0.1	$Ba_{5.7}Sm_{8.2}Ti_{18}O_{54}$	13.5200	21.7692	3.7889	13.5247	22.017	4.14837
0.2	$Ba_{5.4}Sm_{8.4}Ti_{18}O_{54}$	13.5183	21.7605	3.7881	13.5233	22.021	4.12242
0.3	$Ba_{5.1}Sm_{8.6}Ti_{18}O_{54}$	13.5128	21.7585	3.7856	13.5213	22.085	4.11928
0.4	$Ba_{4.8}Sm_{8.8}Ti_{18}O_{54}$	13.4938	21.7534	3.7835	13.5161	22.048	4.16117
0.5	$Ba_{4.5}Sm_{9.0}Ti_{18}O_{54}$	13.4875	21.7521	3.7821	13.5151	22.021	4.1223
0.6	$Ba_{4.2}Sm_{9.2}Ti_{18}O_{54}$	13.4647	21.7502	3.7819	13.5028	22.001	4.1028
0.7	$Ba_{3.9}Sm_{9.4}Ti_{18}O_{54}$	13.4589	21.7499	3.7812	13.4934	22.061	4.1001

Table 3. Ceramic compositions and variation of Lattice constants with sintering times of 2 h and 6 h, respectively for $Ba_{6-3x}Sm_{8+2x}Ti_{18}O_{54}$ compounds with $x = 0.0-0.7$ at 1300°C.

x	Ceramic composition	Lattice Constants					
		2 h			6 h		
		a	b	c	a	b	c
0.0	$Ba_{6.0}Sm_8Ti_{18}O_{54}$	12.5101	22.4662	3.8668	12.672	23.272	4.028
0.1	$Ba_{5.7}Sm_{8.2}Ti_{18}O_{54}$	12.5023	22.4592	3.8526	12.656	23.265	4.001
0.2	$Ba_{5.4}Sm_{8.4}Ti_{18}O_{54}$	12.4938	22.4538	3.8512	12.636	23.234	3.928
0.3	$Ba_{5.1}Sm_{8.6}Ti_{18}O_{54}$	12.4912	22.4212	3.8501	12.620	23.213	3.911
0.4	$Ba_{4.8}Sm_{8.8}Ti_{18}O_{54}$	12.4901	22.4202	3.8483	12.602	23.201	3.892
0.5	$Ba_{4.5}Sm_{9.0}Ti_{18}O_{54}$	12.4882	22.4182	3.8461	12.589	23.198	3.862
0.6	$Ba_{4.2}Sm_{9.2}Ti_{18}O_{54}$	12.4862	22.4172	3.8445	12.567	23.156	3.823
0.7	$Ba_{3.9}Sm_{9.4}Ti_{18}O_{54}$	12.4823	22.4156	3.8414	12.523	23.115	3.801

the morphology. However, with raised sintering time, formation bar-shaped grains originated at the expense of smaller grains, depicted in fig. 3b. Same was the case with the compounds of Gd series, shown in fig. 4b (i, ii). A network of large sized randomly distributed bar-shaped grains was obtained when sintered for 6 h. For the series of Nd, SEMs shown in fig c, depict that with increased sintering time more and more needle-like

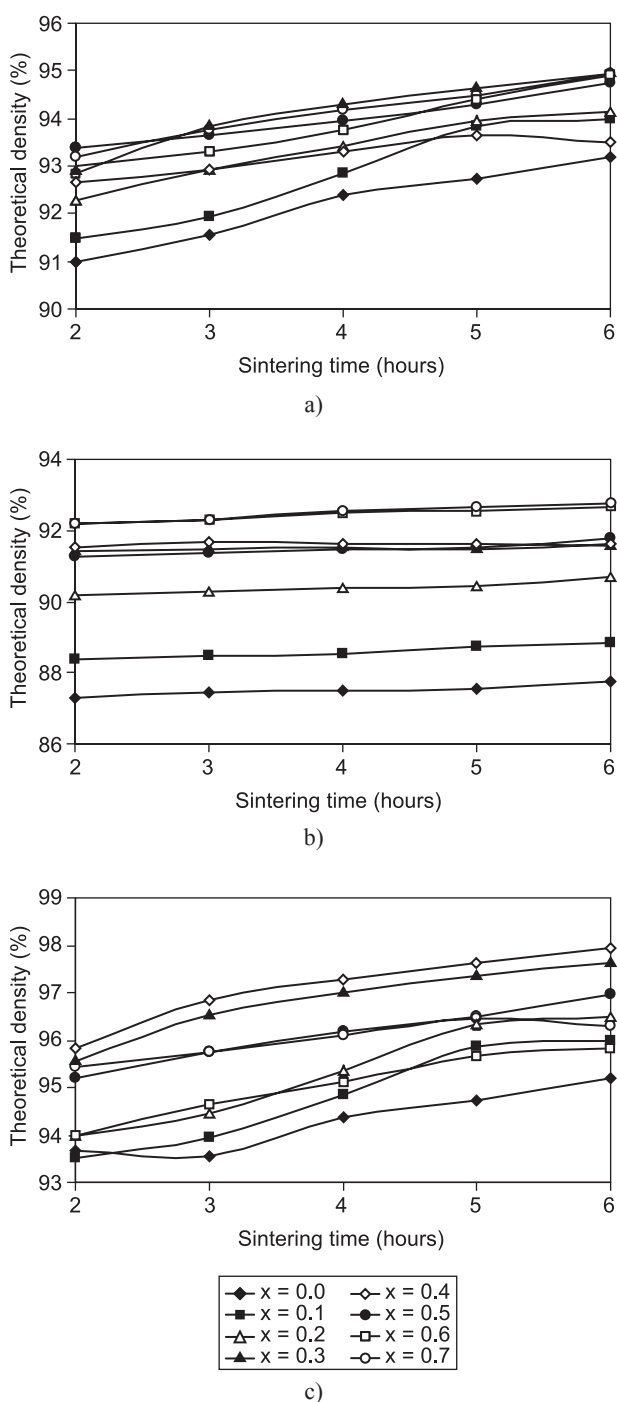


Figure 2. Theoretical density (%) as a function of sintering time for: a) Sm series, b) Gd series, c) Nd series, respectively at 1300°C.

(acicular) grains come into contact increasing the grain boundary area and resulted in grain growth. Again, more fine grains appeared with sintering time of 6 h because long acicular grains grew at the expense of short ones.

Furthermore, the crystallites mean dimension (D) for the three series sintered at different times (2-6 h) and $x = 0.0-0.7$ was estimated using XRD data with the classical Scherrer formula $D(\mu\text{m}) = k\lambda/\cos\Theta$, where β is the full width at half maximum of diffraction peak, Θ is the Bragg angle and k is a constant [19]. It was observed that crystallites mean dimension decreased with increase in sintering times for $\text{Ba}_{6-3x}\text{Sm}_{8+2x}\text{Ti}_{18}\text{O}_{54}$ and $\text{Ba}_{6-3x}\text{Gd}_{8+2x}\text{Ti}_{18}\text{O}_{54}$ series, and increased for $\text{Ba}_{6-3x}\text{Nd}_{8+2x}\text{Ti}_{18}\text{O}_{54}$ series as illustrated in fig. 4. The crystallites dimensions vary between 0.356 and 0.7637 micron for all the series.

Fig. 5 illustrates the relative dielectric constant values as a function of sintering time for the Sm, Gd and Nd series and various x values. ϵ' values were observed to be increased with an increase in sintering time, as shown in fig. 5a-c. Moreover, it was observed that the dielectric constants decreased as the amount of substitution of Ln for Ba increased. Loss tangent ($\tan\delta$) as a function of sintering time for various compositions and the three series is illustrated in fig. 6a-c. Remarkable decrease in the values of tangent loss has been obtained with the raise in sintering time. However, the loss increased with the increase in composition (x) in all the series.

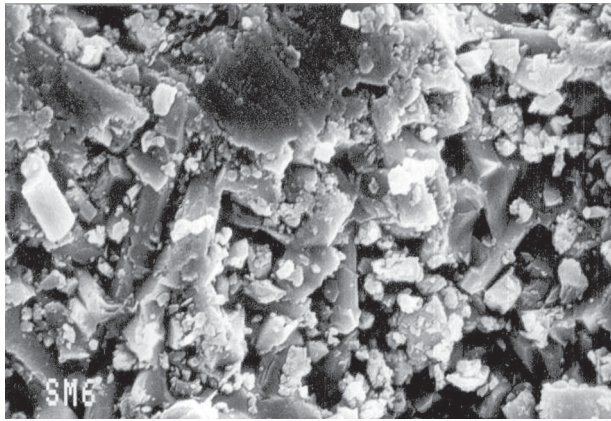
DISCUSSION

Lattice parameters increased with longer sintering times due to the proper crystallization of crystallites. However, the lattice parameters were observed to decrease linearly along a series. The reduction in the values of the lattice parameters might be attributed to the decrease of volume in the octahedra induced by the differences of the ionic radii between Ba and Ln, because the ionic radius of Ln (= Sm, Gd and Nd) is smaller than that of Ba. These changes in a , b and c dimensions were again due to the ionic radii difference of Ba and Ln ions. For the changes per Å, a maximum has been obtained for the c -axis with a minimum for the a -axis. This is attributed to the reason that as the amount of the Ln content increased these medium sized valence cations substituted for Ba & Ti ions. Hence the lattice parameters decreased with Ln substitution. So the variation in the lattice parameters is considered to be caused by the variation in the interatomic distances of octahedral. Therefore, lattice parameters might have decreased when distances decreased.

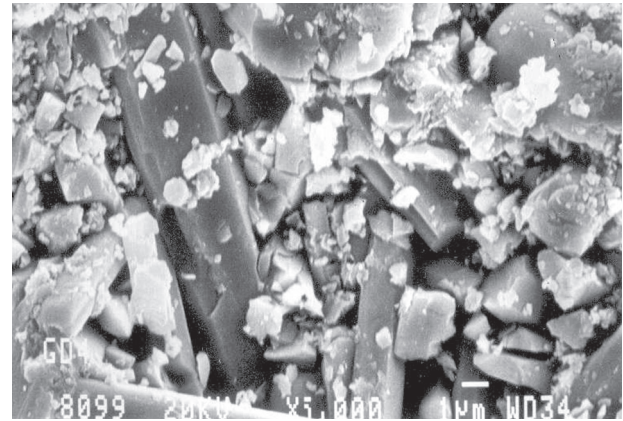
It was deduced that the percentage theoretical density of the compounds of each series increased because during the heat treatment each crystallite got enough dwelling time to get properly crystallized. Moreover, with longer sintering times, the number of pores decreases and hence

the pore size coarsens resulting in an increase in sintered density. The subsequent study of microstructure helps to understand the increased density for prolonged sintering. It was observed in the micro photographs in fig. 3a (i) for Sm series, fired for 2 h, that the sample consisted of several phases of irregular shape randomly distributed, voids and the shorter grains were originally located. This was due to shorter sintering time or improper sintering

schedule. But, it can be seen in fig. 3a (ii), in compounds sintered for 6 h, grains came into contact and their continual growth resulted in the formation of new grains. This caused densification of grains and resulted in the increased density and hence the pores and voids reduced to an extent. Longer sintering time resulted in the growth of grains from central nucleus. With low sintering time, crystallization remains incomplete resulting in pores and

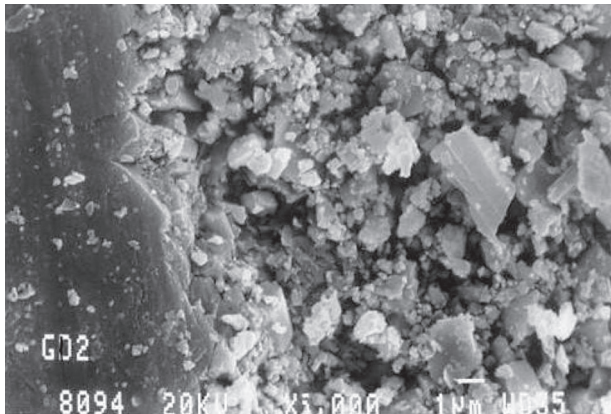


i)

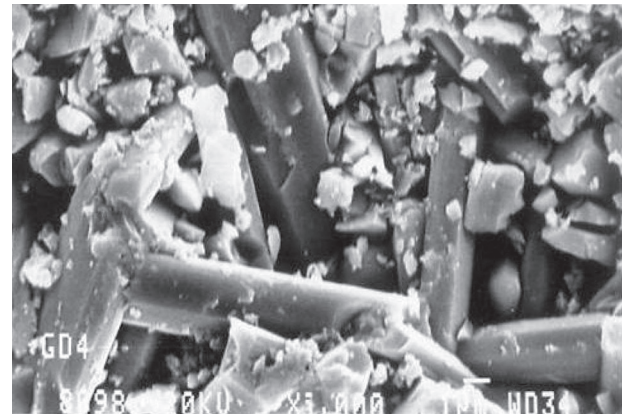


ii)

Figure 3a. Micrographs for $Ba_{6-3x}Sm_{8+2x}Ti_{18}O_{54}$ compounds sintered for (i) 2 h and (ii) 6 h at 1300°C.



i)

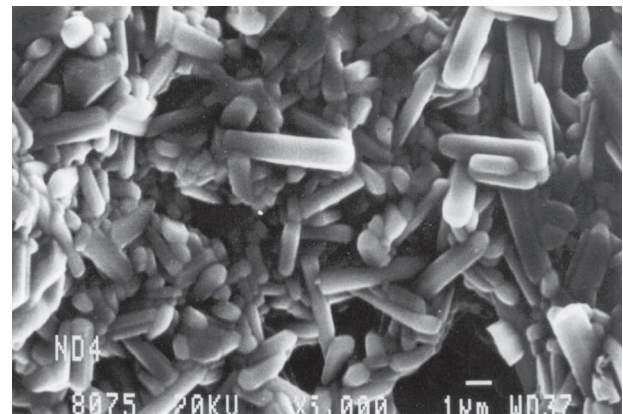


ii)

Figure 3b. Micrographs for $Ba_{6-3x}Gd_{8+2x}Ti_{18}O_{54}$ compounds sintered for (i) 2 h and (ii) 6 h at 1300°C.



i)



ii)

Figure 3c. Micrographs for $Ba_{6-3x}Nd_{8+2x}Ti_{18}O_{54}$ compounds sintered for (i) 2 h and (ii) 6 h at 1300°C.

crystal imperfections. Furthermore, with higher sintering times, the large aggregates bonded by high sizes pores disappeared and hence the crystallites sizes increased as given in fig. 4.

The ϵ' values were observed to be increased with an increase in sintering time, as shown in fig. 5a-c, owing to the increase in densities. This is because the raise of sintering time resulted in more uniform grains. It further deduced that decreased pores and grain boundary areas

reduced the lattice imperfections and increased density and hence ϵ' values. The relationships between dielectric constant and sintering times reveal the same behavior as that between densities and sintering times. ϵ' values increased up to the sintering time of 4 h, then tended to saturate. It might be due to the fact that sintering is faster at higher temperatures because of the increased number of active atoms and available sites. After a certain period of holding time, when all the necessary transport

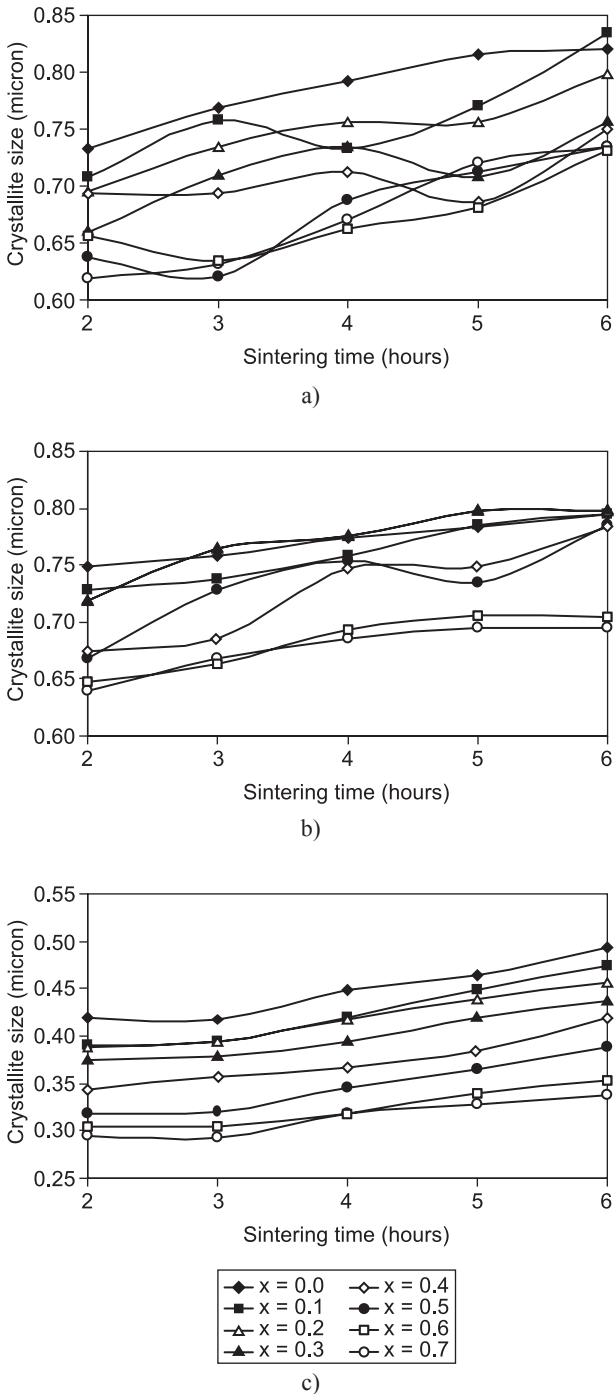


Figure 4. Crystallites size as a function of sintering time for: a) Sm series, b) Gd series, c) Nd series, respectively at 1300°C.

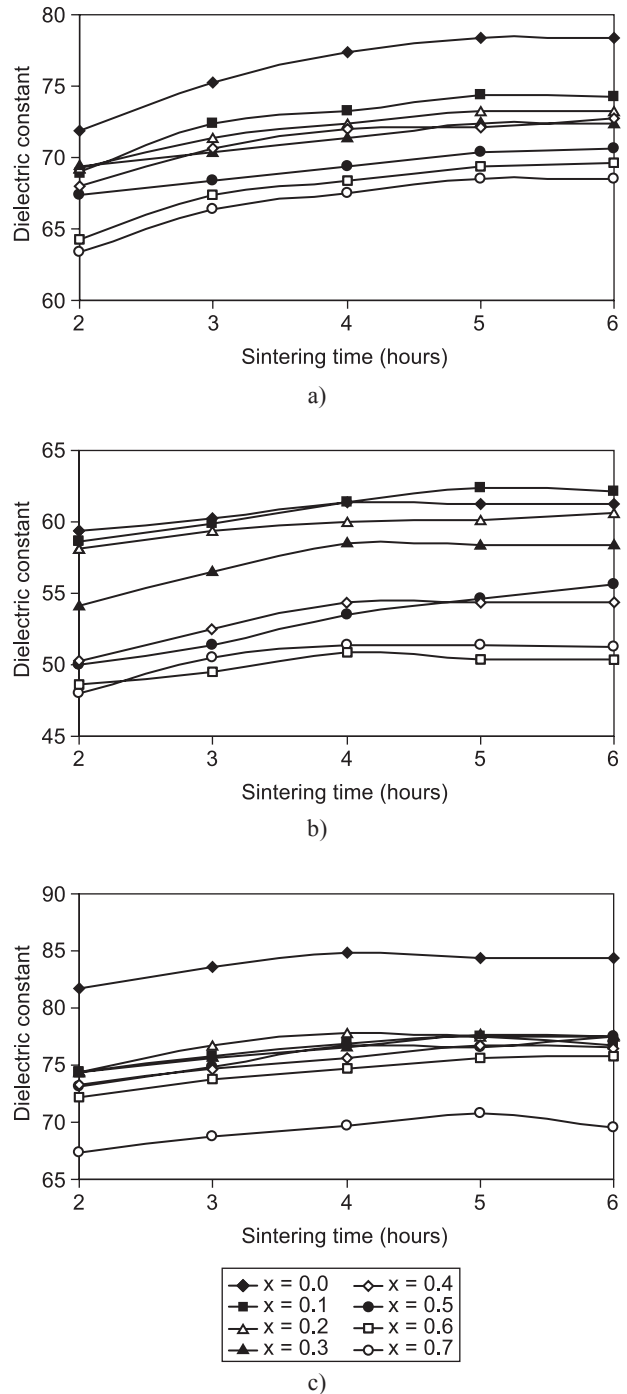


Figure 5. Dielectric constant as a function of sintering time for: a) Sm series, b) Gd series, c) Nd series, respectively at 1300°C and frequency of 3 GHz.

mechanisms would have occurred, there is no effect of increasing the sintering time further. Also, the dielectric constants decreased as the amount of substitution of Ln for Ba increased. It was basically due to the difference in the radii of the substituted ions. When the composition varied, the concentration of Ba decreased and Ln increased according to the formula. Ln ions are middle sized ions and therefore when substituted themselves at the large sized Ba sites, some vacancies might have

created. These became the prime source for the creation of pores and voids, and hence the values of ϵ' decreased. Moreover, the dielectric constant depends on the lattice parameters and the increase of Ti amount might cause the shrinkage of the perovskite octahedral, reducing the values of ϵ' .

Loss tangent decreased with the raise in sintering time. This may be attributed to the stability of the crystal structure induced by the Ln substitution for Ba. Losses are basically dominated by crystal imperfections, oxygen vacancies, grain sizes and densification or porosity. Densification and phase assemblage are the main factors that determine the dielectric losses and can be improved by good sintering times. In this work, proper sintering schedule not only resulted in higher densities, stable crystal structure and high dielectric constants, but dielectric loss tangent was also improved. Also, the loss increased with the increase in composition (x) in all the series due to the creation of more and more vacancies, voids and pores when the Ln ions substituted to Ba sites. Loss tangents also showed the same trends to that observed for densities and dielectric constants. Finally, it was observed that proper sintering schedules greatly improve the quality of dielectrics. Further, when a material with low loss and high dielectric constant is targeted for a specific microwave application, the optimum Ln concentration has always been a compromise between the high ϵ' and low $\tan\delta$.

CONCLUSION

The crystalline phases of $\text{Ba}_{6-3x}\text{Ln}_{8+2x}\text{Ti}_{18}\text{O}_{54}$ compounds with $x = 0.0-0.7$ and Ln = Sm, Gd and Nd were identified in the orthorhombic system with a possible space group of Pbam No. 55 with the help of X-Ray diffraction patterns. SEMs showed that pores and voids reduced with increased sintering times. We concluded that the dielectric properties including densification remarkably improved with longer sintering times. Percentage theoretical densities along with dielectric constants increased while losses decreased with an increase in sintering time. However, ϵ' values decreased and $\tan\delta$ increased with an increased Ln concentration. Proper sintering schedule resulted in stable crystal structure, improved densification and dielectric properties for the three series synthesized.

References

1. Sunatori H., Okamoto T., Takata M.: *J.Ceram. Soc. Jap.* *111*, 217 (2003).
2. Glinchuk M. D., Bykov I. P., Korneinko S. M., Laguta V. V., Slipenyuk A. M., Belous A. G., V'yunovo L. I., Yanchevski O. Z.: *J. Mater.Chem.* *10*, 941 (2000).
3. Lu D. Y., Koda T., Suzuki H., Toda M.: *J. Ceram. Soc. Jap.* *113*, 721 (2005).

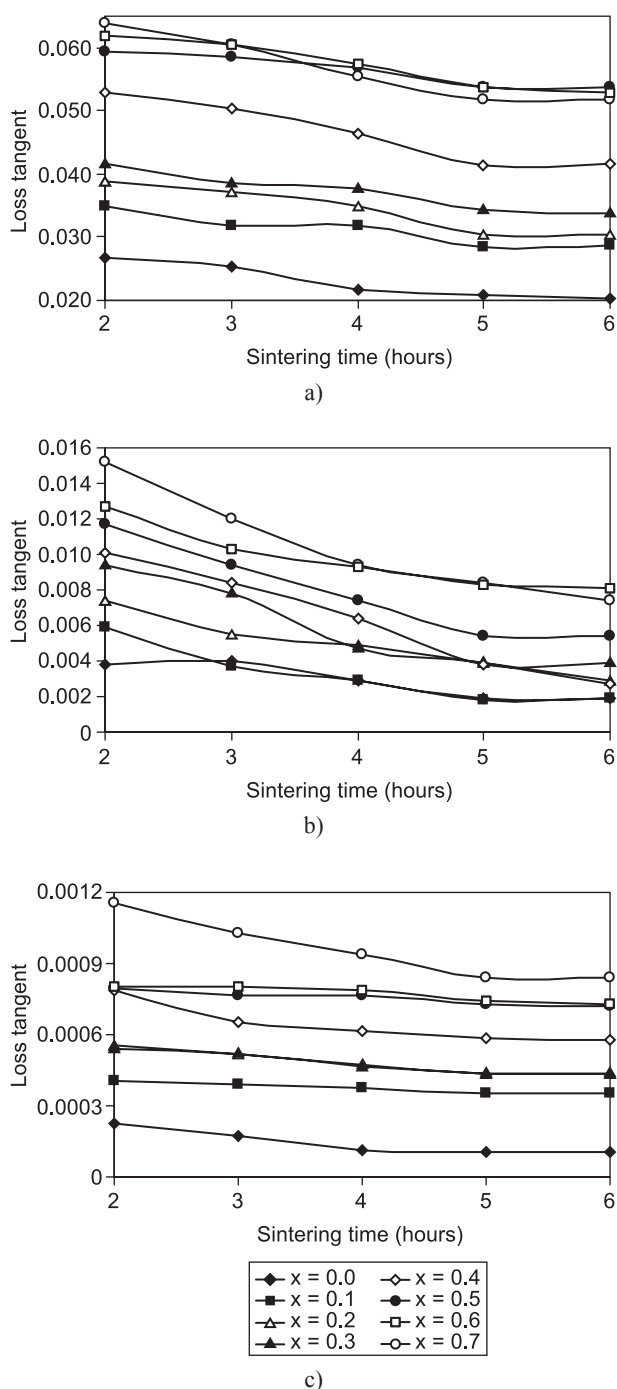


Figure 6. Loss tangent as a function of sintering time for: a) Sm series, b) Gd series, c) Nd series, respectively at 1300°C and frequency of 3 GHz.

4. Kishi H., Mizuno Y., Chazono H.: *Asso. of Asia Paci. Phys. Soc. Bull.* *14*, 1 (2004).
5. Moulson A. J., Herbert J. M.: *Electroceramics: Materials, properties and Applications*, Chapman-Hall, London 1990.
6. Yang C. F.: *Jpn. J. Appl. Phys.* *39*, 1430 (2000).
7. Ohsato H., Kato H., Mizuta M., Nishigaki S., Okuda T.: *Jpn. J. Appl. Phys.* *34*, 5413 (1995).
8. Kolar D., Gaberscek S., Volavsek B., Parker H. S., Roth R. S.: *J. Solid State Chem.* *38*, 158 (1991).
9. Valant M., Suvorov D., Kolar D.: *Jpn. J. Appl. Phys.* *35*, 144 (1996).
10. Ohsato H., Ohhashi T., Okuda T., Sumiya K., Suzuki S.: *Adv. in X-Ray anal.* *37*, 79 (1994).
11. Kaur D., Narang S.B., Singh K.: *Ceram Inter.* *33*, 249 (2006).
12. Kaur D., Narang S.B., Singh K.: *J. Ceram Process Resea.* *7*, 31 (2006).
13. Narang S. B., Kaur D.: *Integ Ferro.* *105*, 87 (2009).
14. Ohsato H.: *J. Eur. Ceram. Soc.* *21*, 2703 (2001).
15. Ohsato H.: *J. Ceram. Soc. Japan* *113*, 703 (2005).
16. Davis J. R.: *Engineered Materials Handbook, Vol 4: Ceramics and Glasses*, ASM International: Metals park OH, 1991.
17. El-rifae A. M.: *J. Ceram. Soc. Jap.* *23*, 93 (2003).
18. Gergs M. K.: *J. Ceram. Soc. Jap.* *30*, 47 (2007).
19. Alexendru H. V., Berbecau C., Ioachim A., Toacsen M. I., Nedelco L., Ghetu D.: *Mater. Sci. and Eng. B* *109*, 152 (2004).